


Article

Simultaneous Estimation of Two Coupled Hydrogen Bond Geometries from Pairs of Entangled NMR Parameters: The Test Case of 4-Hydroxypyridine Anion

Elena Yu. Tupikina ^{1,*} , Mark V. Sigalov ² and Peter M. Tolstoy ¹ ¹ Institute of Chemistry, St. Petersburg State University, 199034 St. Petersburg, Russia; peter.tolstoy@spbu.ru² Department of Chemistry, Ben-Gurion University of the Negev, Beer-Sheva 84105, Israel; msigalov@bgu.ac.il

* Correspondence: e.tupikina@spbu.ru

Abstract: The computational method for estimating the geometry of two coupled hydrogen bonds with geometries close to linear using a pair of spectral NMR parameters was proposed. The method was developed based on the quantum-chemical investigation of 61 complexes with two hydrogen bonds formed by oxygen and nitrogen atoms of the 4-hydroxypyridine anion with OH groups of substituted methanols. The main idea of the method is as follows: from the NMR chemical shifts of nuclei of atoms forming the 4-hydroxypyridine anion, we select such pairs, whose values can be used for simultaneous determination of the geometry of two hydrogen bonds, despite the fact that every NMR parameter is sensitive to the geometry of each of the hydrogen bonds. For these parameters, two-dimensional maps of dependencies of NMR chemical shifts on interatomic distances in two hydrogen bonds were constructed. It is shown that, in addition to chemical shifts of the nitrogen atom and quaternary carbon, which are experimentally difficult to obtain, chemical shifts of the carbons and protons of the CH groups can be used. The performance of the proposed method was evaluated computationally as well on three additional complexes with substituted alcohols. It was found that, for all considered cases, hydrogen bond geometries estimated using two-dimensional correlations differed from those directly calculated by quantum-chemical methods by not more than 0.04 Å.

Keywords: hydrogen bonds; NMR; structure determination

Citation: Tupikina, E.Y.; Sigalov, M.V.; Tolstoy, P.M. Simultaneous Estimation of Two Coupled Hydrogen Bond Geometries from Pairs of Entangled NMR Parameters: The Test Case of 4-Hydroxypyridine Anion. *Molecules* **2022**, *27*, 3923. <https://doi.org/10.3390/molecules27123923>

Academic Editors: Mirosław Jablonski and Liudmil Antonov

Received: 25 April 2022

Accepted: 16 June 2022

Published: 18 June 2022

Publisher's Note: MDPI stays neutral with regard to jurisdictional claims in published maps and institutional affiliations.



Copyright: © 2022 by the authors. Licensee MDPI, Basel, Switzerland. This article is an open access article distributed under the terms and conditions of the Creative Commons Attribution (CC BY) license (<https://creativecommons.org/licenses/by/4.0/>).

1. Introduction

Spectral NMR diagnostics is an important tool for studies of complexes with hydrogen bonds, as oftentimes it is the main way to obtain reliable information about hydrogen bond geometry and strength [1–7]. At the moment, there are a number of correlational equations linking the numerical value of spectral NMR parameters and the geometry/energy of a single hydrogen bond [8]. Some of them are well established and widely used, and their applicability was tested for multiple set of complexes, while others are applicable only to particular complexes and conditions. Among the parameters whose change upon the formation of a hydrogen-bonded complex is correlated with the strength of a X–H...Y hydrogen bond, one can distinguish two major groups. The parameters of the first group are characterized by a monotonous change along the proton transfer coordinate. As representatives of this group, one can name the chemical shifts of heavy nuclei δ_X and δ_Y and the spin–spin coupling constants $^1J_{XH}$ and $^1J_{HY}$ [9–13]. Parameters from the second group exhibit extremal values for the shortest (strongest) hydrogen bond. As an example, one could mention the chemical shift of the bridging proton δ_H or the spin–spin coupling constant $^{2h}J_{XY}$, whose change along the proton transfer coordinate can be characterized by a bell-shaped curve [3–5,14–17]. Parameters from the first group are preferable when solving the inverse spectral problem as their value unequivocally corresponds to a single geometry of a hydrogen bond. For parameters from the second group, there is an uncertainty

that is caused by the fact that a single value of the parameter can be observed for two configurations of a hydrogen bond.

Despite the successful development of numerous methods of spectral diagnostics for estimating the geometry and strength of hydrogen bonds, there are some relevant issues that remain to be solved. For example, it is not known how the inverse spectral problem can be solved for systems with multiple mutually interacting hydrogen bonds, since the magnitude of each spectral parameter can be influenced by the presence of all hydrogen bonds simultaneously.

The aim of this computational work is to demonstrate the possibility of solving the inverse spectral problem for a system with two coupled hydrogen bonds, in particular, to find such pairs of spectral NMR variables that could be used for an unequivocal evaluation of geometries of a pair of mutually influencing hydrogen bonds. As a model system, we consider a 4-hydroxypyridine anion, which can form two hydrogen bonds as a hydrogen bond acceptor (from the oxygen and nitrogen side) with two substituted methanol molecules (Figure 1).

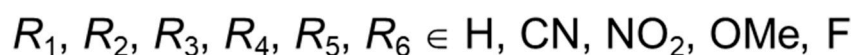
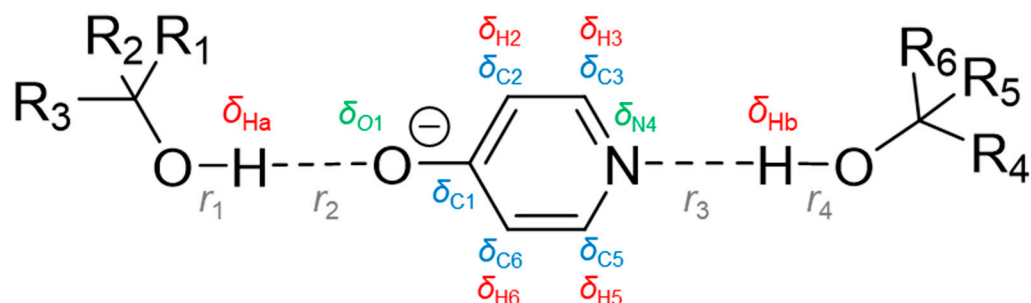


Figure 1. Schematic representation of investigated complexes with two hydrogen bonds formed by 4-hydroxypyridine anion as a hydrogen bond acceptor and two substituted methanols as donors. Geometric parameters (interatomic distances r_1 , r_2 , r_3 and r_4 , grey) and spectral NMR parameters (chemical shifts of bridging protons δ_{Ha} , δ_{Hb} , red; atoms of 4-hydroxypyridine anion's ring: oxygen atom δ_{O1} , green; carbons δ_{C1} , δ_{C2} , δ_{C3} , δ_{C5} , δ_{C6} , blue; hydrogens δ_{H2} , δ_{H3} , δ_{H5} , δ_{H6} , red, and nitrogen δ_{N4} , green) considered in this work are indicated.

Substitution was made by a subsequent replacement of hydrogen atoms by CN, NO₂, OMe or F groups. The resulting set of substituted methanols served as a source of proton donors of various strengths, regardless of their practical chemical stability. Table 1 shows the pattern of substitution used within each of the four sub-series of complexes (full list of substituents can be found in Table S1 in the Supporting Information). Together with the unsubstituted complex $R_1 = R_2 = R_3 = \text{H}$, $R_4 = R_5 = R_6 = \text{H}$, 61 complexes with two hydrogen bonds were considered in this work. In such systems, OHO and OHN hydrogen bonds can be of various strengths (from weak to moderate-strong, it is controlled by the choice of substituents). All hydrogen bonds are fairly linear (the range of OHO and OHN angles is 156°–179°, see Table S1) and are formed along the direction of the lone pair localization on proton-accepting O and N atoms. The central 4-hydroxypyridine anion can be negatively charged (OH...O[−] PyrN...HO), neutral (O[−]...HOPyrN...HO or OH...OPyrNH...O[−]) or even positively charged (O[−]...HOPyrNH⁺...O[−]), depending on proton positions in hydrogen bonds. Therefore, such a choice of model systems is suitable for the investigation of complexes with two mutually influencing hydrogen bonds (OHO and OHN) in a wide range of hydrogen bond geometries formed by neutral or charged species. Throughout the work, parameters associated with the OHO hydrogen bond will be denoted with an index “a” and those of OHN—with an index “b”.

Table 1. List of substituents of 4-hydroxypyridine anion with two cyano-substituted methanol molecules. Pattern of substitution used for the selection of proton donors in complexes shown in Figure 1. X stands for one of the following substituents: CN, NO₂, OMe or F.

R_1	R_2	R_3	R_4	R_5	R_6
H	H	H	X	H	H
H	H	H	X	X	H
H	H	H	X	X	X
X	H	H	H	H	H
X	H	H	X	H	H
X	H	H	X	X	H
X	H	H	X	X	X
X	X	H	H	H	H
X	X	H	X	H	H
X	X	H	X	X	H
X	X	H	X	X	X
X	X	X	H	H	H
X	X	X	X	H	H
X	X	X	X	X	H
X	X	X	X	X	X

The proposed concept for simultaneous solution of the inverse spectral problem for both coupled hydrogen bonds is as follows. In order to determine the geometries of two hydrogen bonds, two spectral parameters are needed. A particular value of a chosen spectral parameter corresponds to multiple combinations of the two hydrogen bond geometries, forming an isoline on a distribution map of a spectral parameter as a function of two proton transfer coordinates (Figure 2, top). However, if one measures two spectral parameters, the intersection of two isolines (Figure 2, bottom) gives the geometry of the two hydrogen bonds in a coupled system. The case with a single intersection of two isolines is preferable and will be used in the following discussion as the criterion for a choice of spectral parameters for solving the inverse spectral problem.

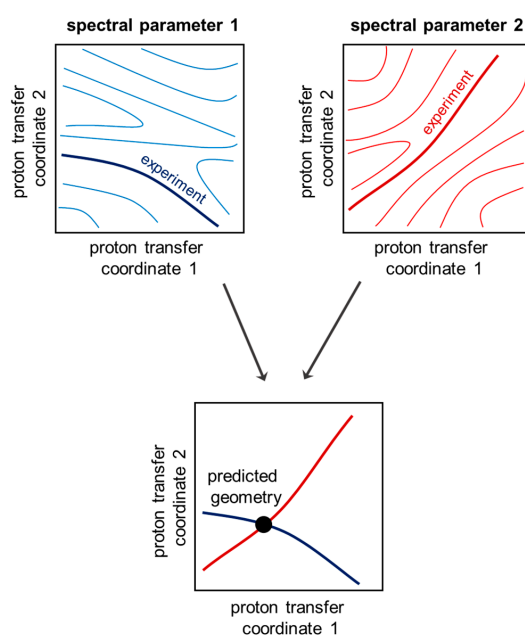


Figure 2. Schematic representation of the algorithm of inverse spectral problem solving. The isolines are drawn arbitrarily and do not correspond to any particular case.

2. Results and Discussion

The geometric parameters (interatomic distances r_1 , r_2 , r_3 and r_4) of hydrogen bonds in investigated complexes are collected in Table S1. The set of complexes covers a wide range of hydrogen bonds geometries—there are complexes without proton transfer in both hydrogen bonds ($\text{OH}\cdots\text{O}^-$ PyrN $\cdots\text{HO}$), complexes with proton transfer in one of the hydrogen bonds ($\text{O}^- \cdots \text{HOPyrN}\cdots\text{HO}$ or $\text{OH}\cdots\text{OPyrNH}\cdots\text{O}^-$) and complexes with two hydrogen bonds with proton transfer ($\text{O}^- \cdots \text{HOPyrNH}^+ \cdots \text{O}^-$). The dependencies of the $q_{2a} = r_1 + r_2$ coordinate on $q_{1a} = 0.5 \cdot (r_1 - r_2)$ for the OHO hydrogen bond and the $q_{2b} = r_4 + r_3$ coordinate on $q_{1b} = 0.5 \cdot (r_4 - r_3)$ for the OHN hydrogen bond are shown in Figure 3. It is seen that the complexes cover a range of q_1 from ca. -0.4 to ca. 0.35 \AA forming a parabolic curve.

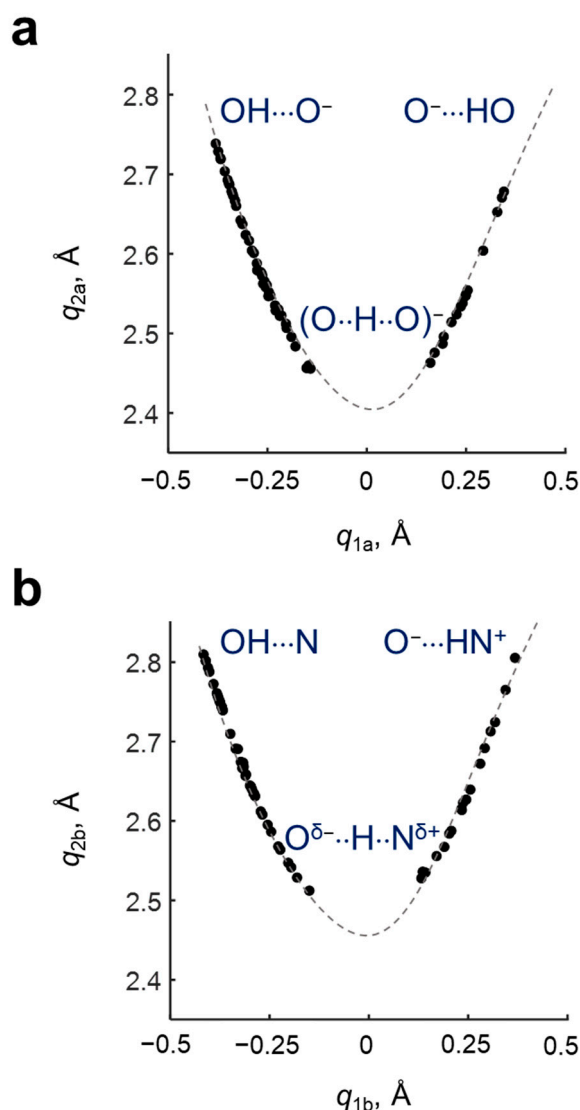


Figure 3. Dependencies of the (a) $q_{2a} = r_1 + r_2$ coordinate on $q_{1a} = 0.5 \cdot (r_1 - r_2)$ for OHO hydrogen bond; dependencies of the (b) $q_{2b} = r_4 + r_3$ coordinate on $q_{1b} = 0.5 \cdot (r_4 - r_3)$ for OHN hydrogen bond. Dashed lines are guides for the eye.

Despite the fact that OHO and OHN hydrogen bonds are divided in space by 4-hydroxypyridine anion, they “feel” the presence of each other through the electronic system of the complex as a whole, the phenomenon is called cooperativity. It manifests as the changes of the proton position in one hydrogen bond depending on the proton position in another hydrogen bond. For example, if one fixes the substituents R_1 , R_2 and

R_3 in the proximity of the OHO hydrogen bond (see a set of points of the same shape and color in Figure 4), the variation of substituents in OHN hydrogen bond causes a change in q_{1a} . Complexes with a “tail-to-tail” ($\text{OH}\cdots\text{O}^- \text{PyrN}\cdots\text{HO}$) and a “head-to-head” ($\text{O}^- \cdots\text{HOPyrNH}^+ \cdots\text{O}^-$) configuration are anti-cooperative (blue areas in Figure 4): i.e., the strengthening of one hydrogen bond causes the weakening of another hydrogen bond. For complexes with “head-to-tail geometry” ($\text{O}^- \cdots\text{HOPyrN}\cdots\text{HO}$ and $\text{OH}\cdots\text{OPyrNH}\cdots\text{O}^-$) (green areas in Figure 4) cooperative effects are observed: i.e., the strengthening of one hydrogen bond causes the strengthening of another. Thus, the character of mutual influence of geometries of OHO and OHN hydrogen bonds in such a system can be either cooperative or anti-cooperative.

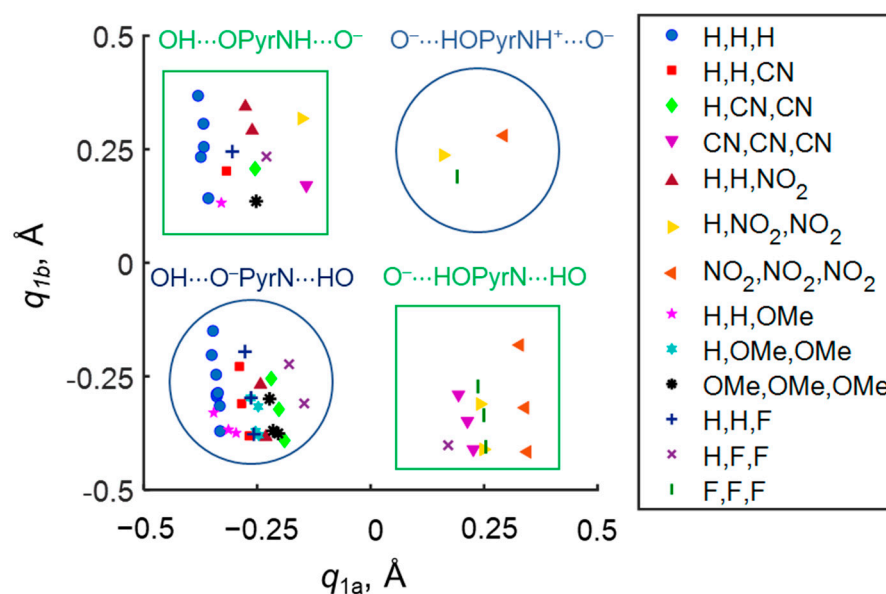


Figure 4. The dependence of proton position in the $\text{NH}\cdots\text{O}$ hydrogen bond q_{1b} on the proton position in the $\text{OH}\cdots\text{O}$ hydrogen bond q_{1a} . The shape and color of a marker indicate a series of complexes with the same set of substituents R_1 , R_2 and R_3 (shown in legend) and varying set of substituents R_4 , R_5 and R_6 . Green areas correspond to cooperative hydrogen bonds and blue areas to anti-cooperative ones.

Among the NMR parameters of the 4-hydroxypyridine anion, which potentially are sensitive to the geometries of $\text{OH}\cdots\text{O}$ and $\text{OH}\cdots\text{N}$ hydrogen bonds, chemical shifts of the nuclei located in the proximity of hydrogen bonds, i.e., carbon (C1) and nitrogen (N4), are the first candidates. The changes of carbon and nitrogen chemical shifts upon complexation, $\Delta\delta_{\text{C1}}$ and $\Delta\delta_{\text{N4}}$, are shown in Figure 5.

In Figure 5, it is clearly seen that the C1 carbon chemical shift changes with the change of geometries of both hydrogen bonds—upon moving the bridging proton along OHO hydrogen bond (with fixed geometry of OHN hydrogen bond), $\Delta\delta_{\text{C1}}$ changes by up to 8 ppm, and moving it along the OHN hydrogen bond causes a change of $\Delta\delta_{\text{C1}}$ by up to 2.5 ppm. In other words, the steepness of the slope of the $\Delta\delta_{\text{C1}}(q_{1a}, q_{1b})$ surface is larger in the direction of q_{1a} than in the direction of q_{1b} . Contrarily, the nitrogen chemical shift is more sensitive to the geometry of the closest (OHN) hydrogen bond. The shape of the isolines of the distributions of $\Delta\delta_{\text{C1}}$ and $\Delta\delta_{\text{N4}}$ makes the unequivocal solving of the inverse spectral problem possible for most cases (except for $q_{1a} \approx -0.3$ Å due to the shape of the $\Delta\delta_{\text{C1}}$ isolines in this region caused by a presence of a hill with its maximal value). Together with the high sensitivity discussed above, this makes the pair $\Delta\delta_{\text{C1}}$ and $\Delta\delta_{\text{N4}}$ quite promising parameters. However, the experimental issues of measuring nitrogen chemical shift (low natural abundance of ^{15}N and line broadening due to quadrupolar interactions in ^{14}N NMR spectra) encourage us to discuss additional NMR parameters.

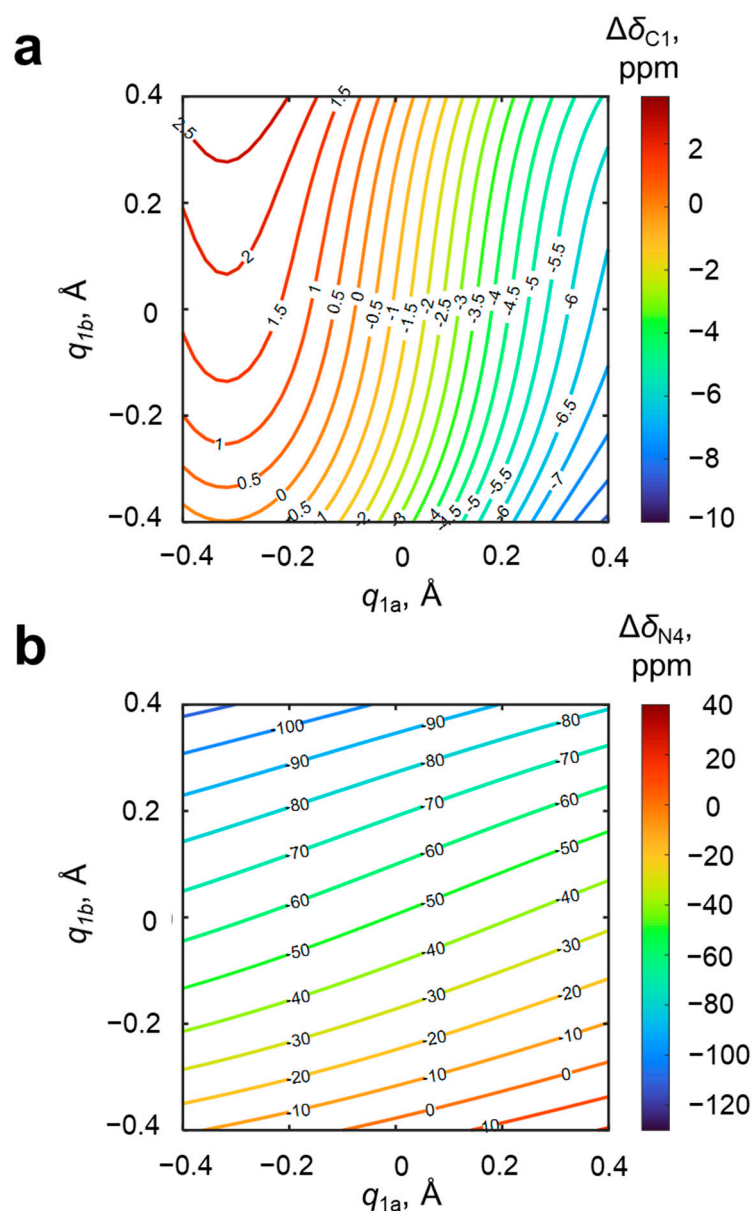


Figure 5. Distributions of the change upon complexation of chemical shift of (a) the C1 atom $\Delta\delta_{C1}$ and (b) the N4 atom $\Delta\delta_{N4}$ along q_1 coordinates for OHO (q_{1a}) and OHN (q_{1b}) hydrogen bonds. The coefficients $a, b_1, c_1, d_1, b_2, c_2$ and d_2 (Equation (1)) and R^2 are given in Table S2. Isolines are drawn with a step of 0.5 and 10 ppm, respectively.

The next pair of “promising” NMR parameters are the changes of chemical shifts of bridging protons in the OHO and OHN hydrogen bonds upon complexation, $\Delta\delta_{Ha}$ and $\Delta\delta_{Hb}$; their dependences on q_{1a} and q_{1b} are shown in Figure 6. Along the OHO hydrogen bond, $\Delta\delta_{Ha}$ increases from 8 to 17 ppm for $q_{1a} < 0$, reaches maximal value at $q_{1a} \approx 0$ and then decreases to 0 ppm. The change of the geometry of the OHN hydrogen bond (q_{1b}) does not significantly influence $\Delta\delta_{Ha}$. A similar situation is observed for $\Delta\delta_{2b}$: moving along the OHN hydrogen bond (q_{1b}) changes $\Delta\delta_{Hb}$ from 9 to 18 ppm for $q_{1b} \approx 0$ and then down to 0 ppm. It is clearly seen that both surfaces have a hill of maximal values of $\Delta\delta_H$ and slopes in the direction of one of q_1 axes (q_{1a} for $\Delta\delta_{Ha}$ and q_{1b} for $\Delta\delta_{Hb}$). It means that the magnitude of the bridging proton chemical shift in a given hydrogen bond is determined almost exclusively by the geometry and electronic features of the three atoms forming this bond. In other words, the chemical shifts of the two bridging protons are not coupled. For the purposes of solving the reverse spectral problem, this is an advantage, because the

magnitude of each chemical shift can be used for the independent evaluation of hydrogen bond geometries.

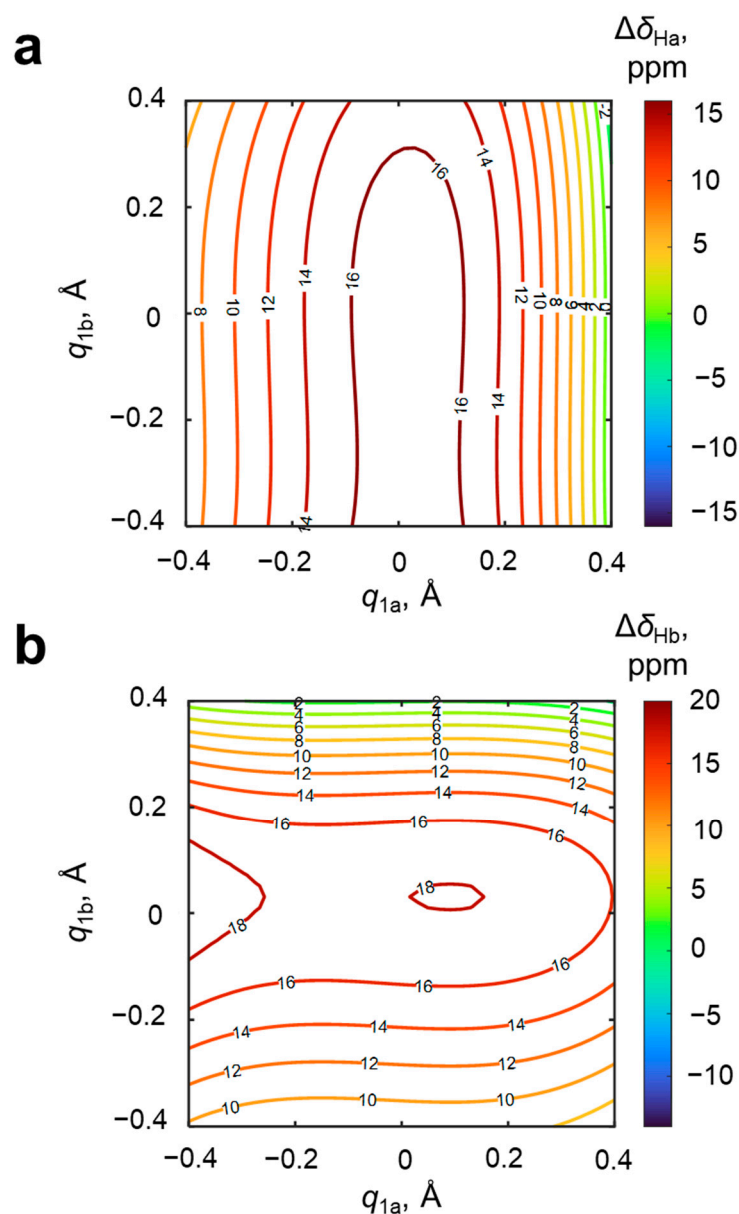


Figure 6. Distributions of the change upon complexation of chemical shift of bridging protons (a) in the OH...O hydrogen bond $\Delta\delta_{\text{Ha}}$ and (b) in the OH...N hydrogen bond $\Delta\delta_{\text{Hb}}$ along q_1 coordinates for OHO (q_{1a}) and OHN (q_{1b}) hydrogen bonds. The coefficients a , b_1 , c_1 , d_1 , b_2 , c_2 and d_2 (Equation (1)) and R^2 are given in Table S2. Isolines are drawn with a step of 2 ppm.

However, there are two principal problems with such an approach. The first problem was mentioned in introduction and is caused by the fact that a particular value of one of the proton chemical shifts ($\Delta\delta_{\text{Ha}}$ or $\Delta\delta_{\text{Hb}}$) corresponds to an isoline in distributions shown in Figure 6a,b that form a hairpin curve. Two hairpin isolines have four intersecting points (see Figure 7), i.e., each set of $\Delta\delta_{\text{Ha}}$ and $\Delta\delta_{\text{Hb}}$ values could correspond to four alternative hydrogen bond geometries. The second problem with using $\Delta\delta_{\text{Ha}}$ and $\Delta\delta_{\text{Hb}}$ for the evaluation of hydrogen bond geometries is due to the fact that, in the experimental spectrum, it is difficult to distinguish which signal will relate to the OHO and which to the OHN hydrogen bond. This issue demands the usage of additional NMR parameters, for example, chemical shifts of the nuclei of 4-hydroxypyridine.

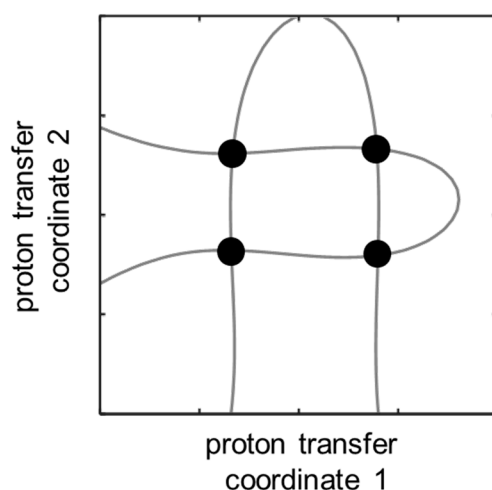


Figure 7. Schematic representation of the non-unequivocal inverse spectral problem solving. The black dots correspond to the four possible solutions. NMR parameters of the 4-hydroxypyridine anion, the chemical shift of carbon δ_{C2} , δ_{C3} , δ_{C5} , δ_{C6} and the hydrogen atoms δ_{H2} , δ_{H3} , δ_{H5} , δ_{H6} , were also analyzed for their sensitivity and applicability for the evaluation of the geometries of OHO and OHN hydrogen bonds. We found that the most promising parameters are arithmetically averaged chemical shifts of C2 and C6 atoms (δ_{C26}), C3 and C5 atoms (δ_{C35}) and H3 and H5 atoms (δ_{H35}). The distributions of changes of these parameters are shown in Figure 8. Both carbon chemical shifts, $\Delta\delta_{C26}$ and $\Delta\delta_{C35}$, are more sensitive to the closest hydrogen bond (OHO and OHN, respectively). The range of values of $\Delta\delta_{C26}$ was about 10 ppm, $\Delta\delta_{C35}$ —15 ppm, which makes both of them suitable for the accurate evaluation of hydrogen bond geometries. The change of δ_{H35} within the change of the OHO and OHN hydrogen bonds geometries slightly exceeded 1 ppm. The topology of these three surfaces is such that almost all combinations of pair of isolines of $\Delta\delta_{C26}$, $\Delta\delta_{C35}$ and $\Delta\delta_{H35}$ have a single intersection point, thus making the solution of an inverse spectral problem unequivocal.

For an additional estimation of the mutual influence of OHO and OHN hydrogen bonds, calculations for two extra sets of systems with a single hydrogen bond were performed (4-hydroxypyridine anion with one substituted methanol from either the oxygen or nitrogen side, 10 complexes in each extra set). The results of NMR calculations (δ_{C26} and δ_{C35}) are presented in Figures S1 and S2 of the Supporting Information. The difference plot between data shown in Figure 8 (system with two coupled hydrogen bonds) and Figures S1 and S2 (hypothetical system with no coupling between hydrogen bond modeled as a sum of systems with a single hydrogen bond) is shown in Figure S3. It is clearly seen that the cooperativity effects on the NMR parameters are substantial (± 2 –4 ppm, making them non-negligible) and non-monotonous. The strongest effects are observed for the configuration $O^- \cdots HOPyrNH^+ \cdots O^-$.

In order to test the approach proposed in this work, we performed additional calculations of structure and NMR parameters for three arbitrarily chosen complexes of 4-hydroxypyridine anion with CH_3CFHOH and CF_3CFHOH molecules: **1** ($CH_3CFHOH \cdots^- OPyrN \cdots HOCFHCF_3$), **2** ($CF_3CFHOH \cdots^- OPyrN \cdots HOCFHCF_3$) and **3** ($CF_3CFHOH \cdots^- OPyrN \cdots HOCFHCH_3$); the optimized structures of **1–3** are shown in Figure 9. The results of the comparison of the “predicted” geometry based on pairs of NMR chemical shifts and the “real” (calculated) geometries of the two hydrogen bonds are summarized in Table 2 and shown in Figures S4–S6 in the Supporting Information. It can be concluded that hydrogen bond geometries estimated using two-dimensional correlations differ from those directly calculated by quantum-chemical methods by not more than 0.04 Å. The only exception is complex **3** (CF_3CFHOH and CF_3CFHOH), for which the chemical shifts of carbons C2 and C6 differ significantly due to the presence of an additional hydrogen bond between the CH-group of the 4-hydroxypyridine anion and the fluorine atom of the substituted methanol (see Figure S7). In this case, using the chemical shift of carbon atom not involved

in additional hydrogen bonding instead of the arithmetically averaged chemical shift $\Delta\delta_{C26}$ is more appropriate.

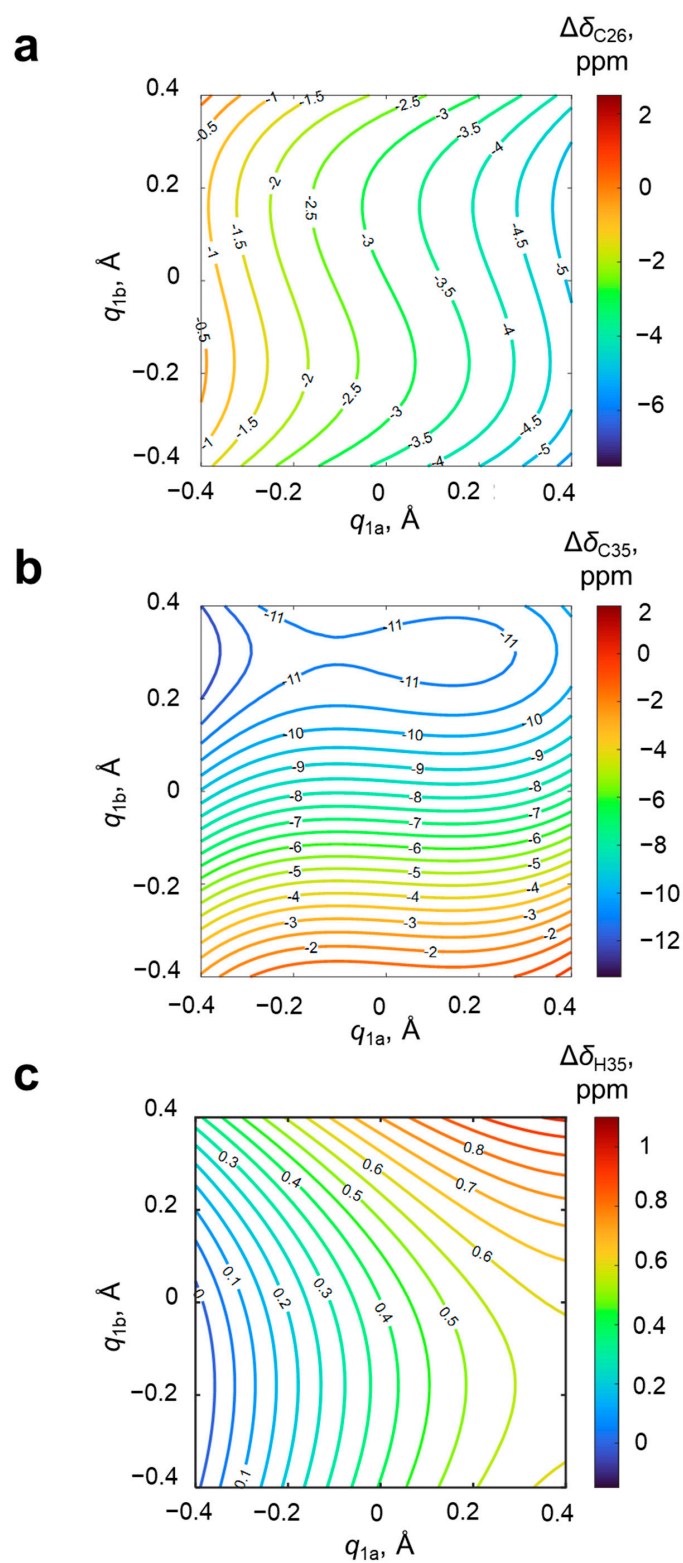


Figure 8. Distributions of the change upon complexation of average chemical shift of (a) C2 and C6 atoms $\Delta\delta_{C26}$, (b) C3 and C5 atoms $\Delta\delta_{C35}$ and (c) H3 and H5 atoms $\Delta\delta_{H35}$ along q_1 coordinates for OHO (q_{1a}) and OHN (q_{1b}) hydrogen bonds. The coefficients $a, b_1, c_1, d_1, b_2, c_2$ and d_2 (Equation (1)) and R^2 are given in Table S2. Isolines are drawn with a step of 0.5 ppm for (a,b) and 0.05 ppm for (c), respectively.

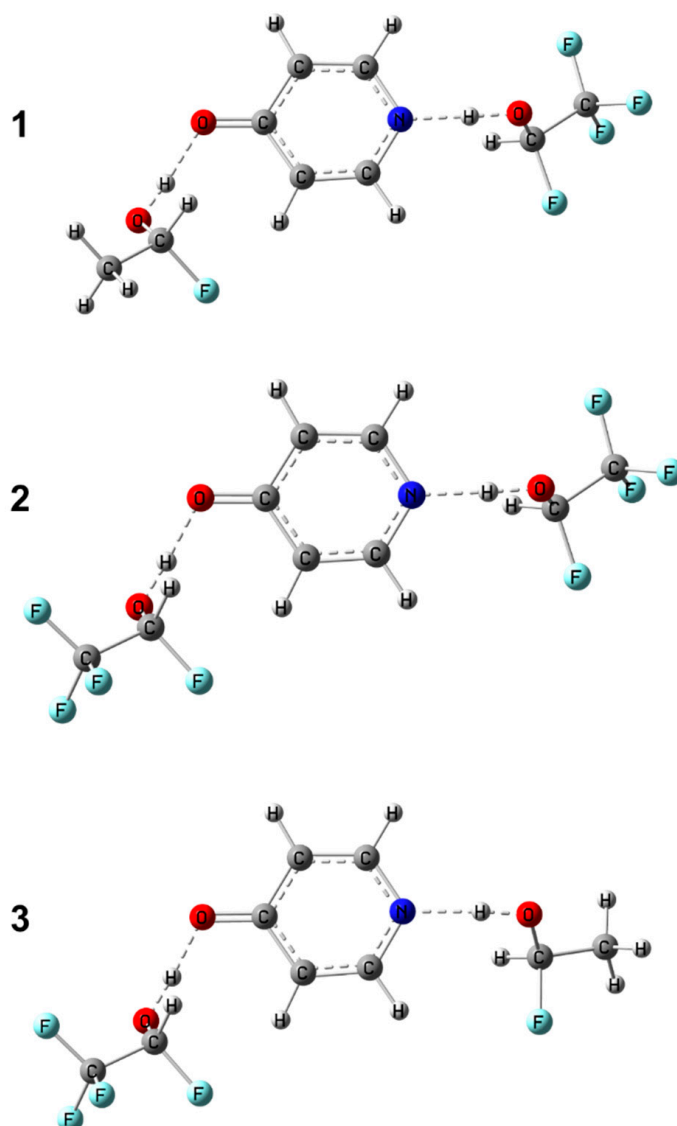


Figure 9. Structures of additional complexes with two hydrogen bonds formed by 4-hydroxypyridine anion as a hydrogen bond acceptor and two substituted methanols as donors used for testing the proposed approach. From top to bottom: **1** (proton donors CH₃CHFOH, CF₃CHFOH), **2** (proton donors CH₃CHFOH, CF₃CHFOH), **3** (proton donors CF₃CHFOH, CH₃CHFOH).

Table 2. Results of testing the proposed approach for three additional complexes, shown in Figure 8: **1** (proton donors CH₃CHFOH, CF₃CHFOH), **2** (proton donors CH₃CHFOH, CF₃CHFOH), **3** (proton donors CF₃CHFOH, CH₃CHFOH).

Complex (Proton Donors)	Calculated Geometry	Pair of Parameters for Prediction	Predicted Geometry
1 (CH ₃ CHFOH, CF ₃ CHFOH)	$q_{1a} = -0.27 \text{ \AA}$, $q_{1b} = -0.20 \text{ \AA}$	$\Delta\delta_{C1} = 1.2 \text{ ppm}$, $\Delta\delta_{N4} = -37.0 \text{ ppm}$	$q_{1a} = -0.29 \text{ \AA}$, $q_{1b} = -0.21 \text{ \AA}$
		$\Delta\delta_{C26} = -1.2 \text{ ppm}$, $\Delta\delta_{C35} = -5.5 \text{ ppm}$,	$q_{1a} = -0.30 \text{ \AA}$, $q_{1b} = -0.17 \text{ \AA}$
		$\Delta\delta_{C35} = -5.5 \text{ ppm}$, $\Delta\delta_{H35} = 0.03 \text{ ppm}$	$q_{1a} = -0.32 \text{ \AA}$, $q_{1b} = -0.19 \text{ \AA}$

Table 2. Cont.

Complex (Proton Donors)	Calculated Geometry	Pair of Parameters for Prediction	Predicted Geometry
2 (CF ₃ CHFOH, CF ₃ CHFOH)	$q_{1a} = -0.19 \text{ \AA}$, $q_{1b} = -0.23 \text{ \AA}$	$\Delta\delta_{C1} = 0.6 \text{ ppm}$, $\Delta\delta_{N4} = -29.4 \text{ ppm}$	$q_{1a} = -0.20 \text{ \AA}$, $q_{1b} = -0.23 \text{ \AA}$
		$\Delta\delta_{C26} = -2.2 \text{ ppm}$, $\Delta\delta_{C35} = -4.6 \text{ ppm}$,	$q_{1a} = -0.15 \text{ \AA}$, $q_{1b} = -0.20 \text{ \AA}$
		$\Delta\delta_{C35} = -4.6 \text{ ppm}$, $\Delta\delta_{H35} = 0.22 \text{ ppm}$	$q_{1a} = -0.18 \text{ \AA}$, $q_{1b} = -0.20 \text{ \AA}$
3 (CF ₃ CHFOH, CH ₃ CHFOH)	$q_{1a} = -0.17 \text{ \AA}$, $q_{1b} = -0.31 \text{ \AA}$	$\Delta\delta_{C1} = 0.0 \text{ ppm}$, $\Delta\delta_{N4} = -14.8 \text{ ppm}$	$q_{1a} = -0.20 \text{ \AA}$, $q_{1b} = -0.33 \text{ \AA}$
		$\Delta\delta_{C26} = -3.0 \text{ ppm}$, $\Delta\delta_{C35} = -3.0 \text{ ppm}$,	$q_{1a} = -0.01 \text{ \AA}$, $q_{1b} = -0.28 \text{ \AA}$
		$\Delta\delta_{C35} = -3.0 \text{ ppm}$, $\Delta\delta_{H35} = 0.24 \text{ ppm}$	$q_{1a} = -0.16 \text{ \AA}$, $q_{1b} = -0.27 \text{ \AA}$

3. Computational Details

Geometry optimization was performed using second-order Moller–Plesset perturbation theory (MP2) [12,13] with Dunning’ correlation-consistent polarized double- ζ basis set with diffuse functions aug-cc-pVDZ [14]. All calculated geometries were checked for the absence of imaginary frequencies. Chemical shieldings were calculated using DFT (B3LYP) with the augmented polarization consistent triple- ζ basis set aug-pcS-2, which is specially designed for the calculation of shieldings at the DFT level with a high accuracy [18].

Calculations were carried out using the Gaussian16 software. Computational resources were provided by the Computer Center of Saint Petersburg University Research Park (<http://www.cc.spbu.ru/>, accessed on 1 April 2020).

Visualization was performed in GaussView 6.0 and MATLAB 2021b software packages.

For the description of the geometries of OHO and OHN hydrogen bonds, the parameters q_1 and q_2 were used [2,16,17]: $q_1 = 0.5 \cdot (r_{OH} - r_{HY})$, $q_2 = r_{OH} + r_{HY}$, where Y = O, N. The meaning of q_1 and q_2 coordinates is pretty clear for linear hydrogen bonds—the q_1 coordinate is the shift of the hydrogen atom from the hydrogen bond center, the q_2 coordinate is the total length of the hydrogen bond (for strictly linear hydrogen bonds, q_2 is the distance between the heavy atoms O...O or O...N; it should be noted that, as hydrogen bonds deviate from linearity, q_2 loses this geometrical meaning, because in this case q_2 is slightly longer than the distance O...O or O...N). For the OHO hydrogen bond, the following pair of coordinates was used $q_{1a} = 0.5 \cdot (r_1 - r_2)$ and $q_{2a} = r_1 + r_2$ and for OHN, they were $q_{1b} = 0.5 \cdot (r_4 - r_3)$ and $q_{2b} = r_4 + r_3$, respectively.

The algorithm of construction for the distributions of spectral parameters ($\Delta\delta_{C1}$, $\Delta\delta_{N4}$ and others discussed in this work) along the q_{1a} and q_{1b} was as follows. For a set of complexes shown in Figure 1, NMR parameters were calculated. Let us denote the spectral parameter as f . The value of a change of a spectral parameter upon complexation is defined as $\Delta f = f_{\text{complex}} - f_{\text{free}}$ (where f_{free} is the value of a given spectral parameter for an isolated 4-hydroxypyridine anion or methanol, and f_{complex} is the value of the same parameter within a hydrogen-bonded complex). Calculated Δf values were approximated as a function of q_{1a} and q_{1b} using the Curve Fitting Tool implemented in the MATLAB 2021b software package by a polynomial function of a third-degree along q_{1a} and q_{1b} without cross-terms:

$$\Delta f(q_{1a}, q_{1b}) = a + b_1 q_{1a} + c_1 q_{1a}^2 + d_1 q_{1a}^3 + b_2 q_{1b} + c_2 q_{1b}^2 + d_2 q_{1b}^3 \quad (1)$$

The coefficients a , b_1 , c_1 , d_1 , b_2 , c_2 and d_2 for all discussed parameters and the coefficient of determination R^2 for each approximation are given in Table S2 in the Supporting Information. The resulting functions were plotted as contour plots, in which each isoline

corresponds to the particular value of Δf and is marked by a color and an isovalue for clarity in the following figures. The polynomials were taken as one of the simplest forms that could describe the strongly non-monotonous behavior of spectral parameters. There is no deeper reason for this choice, and for the fitting purposes, other functions could be selected if the data points would allow doing so.

4. Conclusions

In this work, the possibility of solving the inverse spectral problem for a system with two coupled hydrogen bonds was demonstrated on the example of 61 complexes formed by 4-hydroxypyridine anion with two substituted methanols with OHO and OHN hydrogen bonds. The algorithm for using two-dimensional correlations is as follows: for measured or calculated change of two given spectral parameters, one should find isolines on their corresponding plots and overlap them (see Figure 2). The coordinates of the intersection point of the two isolines will give the proton positions in both hydrogen bonds. It was demonstrated that any pair of parameters $\Delta\delta_{N4}$, $\Delta\delta_{C1}$, $\Delta\delta_{C26}$, $\Delta\delta_{C35}$ and $\Delta\delta_{H35}$ is suitable for the evaluation of hydrogen bond geometries. However, $\Delta\delta_{C1}$, $\Delta\delta_{C26}$, $\Delta\delta_{C35}$ and $\Delta\delta_{H35}$ are more easily available from an experiment.

Thus far, we have only tested our approach computationally on three examples of complexes. The applicability of the method “in practice” awaits experimental verification by future researchers. Indeed, the proposed approach has obvious limitations. Firstly, such 2D maps are constructed for each compound individually (in our case for 4-hydroxypyridine anion). Secondly, the experimental application of the approach requires the measurements of signals that are not averaged out by fast (in the NMR time scale) molecular exchange—a condition that is not necessarily satisfied for intermolecular complexes. The coexistence of several types of molecular complexes in a solution at the same time can also complicate the solving of the reverse spectral problem. Thirdly, the accuracy of the 2D chemical shift maps worsens in the presence of additional non-covalent interactions between the proton donors and the central proton-accepting molecule. Fourthly, for other systems, multiple extrema in the 2D maps of spectral parameters can make determination of hydrogen bonds geometries non-unequivocal, as shown in Figure 7. An unfortunate combination of all four factors could, of course, render the proposed approach totally unreliable. Nevertheless, we have shown in principle that, for systems where these limitations are absent or can be neglected, the NMR spectral data can be sufficient to solve the two-dimensional reverse spectral problem even with a significant entanglement of spectral parameters.

The accuracy of geometry estimations with this approach for systems with two OHO and OHN hydrogen bonds (and without additional interactions) is in the range $\pm 0.04 \text{ \AA}$.

Supplementary Materials: The following supporting information can be downloaded at: <https://www.mdpi.com/article/10.3390/molecules27123923/s1>, Table S1: Geometric parameters of OHO and OHN hydrogen bonds; Table S2: Coefficients a , b_1 , c_1 , d_1 , b_2 , c_2 and d_2 for each discussed spectral parameter, R^2 for each approximation; Figure S1: $\Delta\delta_{C35}$ for complexes of hydroxypyridine anion with a single substituted methanol molecule from an oxygen side (OHO hydrogen bond) $\Delta\delta_{C35a}$ and from a nitrogen site (OHN hydrogen bond) $\Delta\delta_{C35b}$. Distributions of the sum $\Delta\delta_{C35} = \Delta\delta_{C35a} + \Delta\delta_{C35b}$ along q_{1a} and q_{1b} hydrogen bonds; Figure S2: $\Delta\delta_{C26}$ for complexes of hydroxypyridine with a single substituted methanol molecule from an oxygen side (OHO hydrogen bond) $\Delta\delta_{C26a}$ and from a nitrogen site (OHN hydrogen bond) $\Delta\delta_{C26b}$. Distributions of the sum $\Delta\delta_{C26} = \Delta\delta_{C26a} + \Delta\delta_{C26b}$ along q_{1a} and q_{1b} hydrogen bonds; Figure S3: $\Delta\delta_{C26} - \Delta\delta_{C35}$ along q_{1a} and q_{1b} ; Figure S4: Solution of the inverse spectral problem for $R_1 = H$, $R_2 = F$, $R_3 = CH_3$, $R_4 = H$, $R_5 = F$, $R_6 = CF_3$; Figure S5: Solution of the inverse spectral problem for $R_1 = H$, $R_2 = F$, $R_3 = CF_3$, $R_4 = H$, $R_5 = F$, $R_6 = CF_3$; Figure S6: Solution of the inverse spectral problem for $R_1 = H$, $R_2 = F$, $R_3 = CF_3$, $R_4 = H$, $R_5 = F$, $R_6 = CH_3$; Figure S7: Optimized geometry of complex 3 with CF_3CFOH and CH_3CFHOH as hydrogen bond donors.

Author Contributions: Conceptualization, P.M.T. and M.V.S.; methodology, E.Y.T.; validation, P.M.T. and M.V.S.; formal analysis, E.Y.T. and M.V.S.; investigation, E.Y.T. and M.V.S.; data curation, E.Y.T.; writing—original draft preparation, E.Y.T.; writing—review and editing, P.M.T. and M.V.S.; visualiza-

tion, E.Y.T.; funding acquisition, P.M.T. All authors have read and agreed to the published version of the manuscript.

Funding: This research was funded by Russian Science Foundation grant number 18-13-00050.

Institutional Review Board Statement: Not applicable.

Informed Consent Statement: Not applicable.

Data Availability Statement: Data is contained within the article or Supplementary Material.

Acknowledgments: This study was supported by the Russian Science Foundation.

Conflicts of Interest: The authors declare no conflict of interest.

Sample Availability: Samples of the compounds are not available from the authors.

References

1. Arunan, E.; Desiraju, G.R.; Klein, R.A.; Sadlej, J.; Scheiner, S.; Alkorta, I.; Clary, D.C.; Crabtree, R.H.; Dannenber, J.J.; Hobza, P.; et al. Definition of the Hydrogen Bond (IUPAC Recommendations 2011). *Pure Appl. Chem.* **2011**, *83*, 1637–1641. [[CrossRef](#)]
2. Jeffrey, G.A.; Yeon, Y. The Correlation between Hydrogen-Bond Lengths and Proton Chemical Shifts in Crystals. *Acta Crystallogr. Sect. B Struct. Sci.* **1986**, *42*, 410–413. [[CrossRef](#)]
3. Lorente, P.; Shenderovich, I.G.; Golubev, N.S.; Denisov, G.S.; Buntkowsky, G.; Limbach, H.-H. ¹H/¹⁵N NMR Chemical Shielding, Dipolar ¹⁵N,²H Coupling and Hydrogen Bond Geometry Correlations in a Novel Series of Hydrogen-Bonded Acid-Base Complexes of Collidine with Carboxylic Acids. *Org. Magn. Reson.* **2001**, *39*, S18–S29. [[CrossRef](#)]
4. Benedict, H.; Shenderovich, I.G.; Malkina, O.L.; Malkin, V.G.; Denisov, G.S.; Golubev, N.S.; Limbach, H.H. Nuclear Scalar Spin-Spin Couplings and Geometries of Hydrogen Bonds. *J. Am. Chem. Soc.* **2000**, *122*, 1979–1988. [[CrossRef](#)]
5. Limbach, H.-H.; Tolstoy, P.M.; Pérez-Hernández, N.; Guo, J.; Shenderovich, I.G.; Denisov, G.S. OHO Hydrogen Bond Geometries and NMR Chemical Shifts: From Equilibrium Structures to Geometric H/D Isotope Effects, with Applications for Water, Protonated Water, and Compressed Ice. *Isr. J. Chem.* **2009**, *49*, 199–216. [[CrossRef](#)]
6. Tupikina, E.Y.; Denisov, G.S.; Melikova, S.M.; Kucherov, S.Y.; Tolstoy, P.M. New Look at the Badger-Bauer Rule: Correlations of Spectroscopic IR and NMR Parameters with Hydrogen Bond Energy and Geometry. FHF Complexes. *J. Mol. Struct.* **2018**, *1164*, 129–136. [[CrossRef](#)]
7. Giba, I.S.; Tolstoy, P.M. Self-Assembly of Hydrogen-Bonded Cage Tetramers of Phosphonic Acid. *Symmetry* **2021**, *13*, 258. [[CrossRef](#)]
8. Tolstoy, P.M.; Tupikina, E.Y. IR and NMR Spectral Diagnostics of Hydrogen Bond Energy and Geometry. In *Spectroscopy and Computation of Hydrogen-Bonded Systems*; Wojcik, M.J., Ozaki, Y., Eds.; Wiley: Hoboken, NJ, USA, 2022.
9. Ando, S.; Ando, I.; Shoji, A.; Ozaki, T. Intermolecular Hydrogen-Bonding Effect on Carbon-13 NMR Chemical Shifts of Glycine Residue Carbonyl Carbons of Peptides in the Solid State. *J. Am. Chem. Soc.* **2002**, *110*, 3380–3386. [[CrossRef](#)]
10. Guo, J.; Tolstoy, P.M.; Koeppe, B.; Golubev, N.S.; Denisov, G.S.; Smirnov, S.N.; Limbach, H.H. Hydrogen Bond Geometries and Proton Tautomerism of Homoconjugated Anions of Carboxylic Acids Studied via H/D Isotope Effects on ¹³C NMR Chemical Shifts. *J. Phys. Chem. A* **2012**, *116*, 11180–11188. [[CrossRef](#)] [[PubMed](#)]
11. Mulloyarova, V.V.; Giba, I.S.; Denisov, G.S.; Ostras', A.S.; Tolstoy, P.M. Conformational Mobility and Proton Transfer in Hydrogen-Bonded Dimers and Trimers of Phosphinic and Phosphoric Acids. *J. Phys. Chem. A* **2019**, *123*, 6761–6771. [[CrossRef](#)] [[PubMed](#)]
12. Tolstoy, P.M.; Smirnov, S.N.; Shenderovich, I.G.; Golubev, N.S.; Denisov, G.S.; Limbach, H.H. NMR Studies of Solid State—Solvent and H/D Isotope Effects on Hydrogen Bond Geometries of 1:1 Complexes of Collidine with Carboxylic Acids. *J. Mol. Struct.* **2004**, *700*, 19–27. [[CrossRef](#)]
13. Del Bene, J.E.; Bartlett, R.J.; Elguero, J. Interpreting 2hJ(F,N), 1hJ(H,N) and 1J(F,H) in the Hydrogen-Bonded FH–Collidine Complex. *Magn. Reson. Chem.* **2002**, *40*, 767–771. [[CrossRef](#)]
14. Harris, T.K.; Zhao, Q.; Mildvan, A.S. NMR Studies of Strong Hydrogen Bonds in Enzymes and in a Model Compound. *J. Mol. Struct.* **2000**, *552*, 97–109. [[CrossRef](#)]
15. Del Bene, J.E.; Alkorta, I.; Elguero, J. Spin-spin coupling across intramolecular N-H+–N hydrogen bonds in models for proton sponges: An ab initio investigation. *Magn. Reson. Chem.* **2008**, *46*, 457–463. [[CrossRef](#)] [[PubMed](#)]
16. Del Bene, J.E.; Elguero, J. Systematic Ab Initio Study of ¹⁵N ¹⁵N and ¹⁵N ¹H Spin-Spin Coupling Constants across N-H +–N Hydrogen Bonds: Predicting N–N and N–H Coupling Constants and Relating Them to Hydrogen Bond Type. *J. Phys. Chem. A* **2006**, *110*, 7496–7502. [[CrossRef](#)] [[PubMed](#)]
17. Shenderovich, I.G.; Tolstoy, P.M.; Golubev, N.S.; Smirnov, S.N.; Denisov, G.S.; Limbach, H.H. Low-Temperature NMR Studies of the Structure and Dynamics of a Novel Series of Acid-Base Complexes of HF with Collidine Exhibiting Scalar Couplings across Hydrogen Bonds. *J. Am. Chem. Soc.* **2003**, *125*, 11710–11720. [[CrossRef](#)] [[PubMed](#)]
18. Jensen, F. Basis Set Convergence of Nuclear Magnetic Shielding Constants Calculated by Density Functional Methods. *J. Chem. Theory Comput.* **2008**, *4*, 719–727. [[CrossRef](#)] [[PubMed](#)]